27 cy
24 to NTIS

ORNL/TM-6878

Effects of Alternate Fuels Report No. 7: Analysis of Failure of a Mullite-Based Refractory Brick in an Industrial Oil-Fired Burner

J. I. Federer
V. J. Tennery

MASTER

OAK RIDGE NATIONAL LABORATORY
OPERATED BY UNION CARBIDE CORPORATION · FOR THE DEPARTMENT OF ENERGY

DISCLAIMER

Printed in the United States of America. Available from
National Technical Information Service
U.S. Department of Commerce
5285 Port Royal Road, Springfield, Virginia 22161
Price: Printed Copy $4.50; Microfiche $3.00

ORNL/TM-6878

Contract No. W-7405-eng-26

METALS AND CERAMICS DIVISION

EFFECTS OF ALTERNATE FUELS REPORT NO. 7: ANALYSIS OF FAILURE OF A MULLITE-BASED REFRACTORY BRICK IN AN INDUSTRIAL OIL-FIRED BURNER

J. I. Federer and V. J. Tennery

Date Published: July 1979

Prepared for
Division of Industrial Energy Conservation
Department of Energy

NOTICE This document contains information of a preliminary nature. It is subject to revision or correction and therefore does not represent a final report.

OAK RIDGE NATIONAL LABORATORY
Oak Ridge, Tennessee 37830
operated by
UNION CARBIDE CORPORATION
for the
DEPARTMENT OF ENERGY

THIS PAGE
WAS INTENTIONALLY
LEFT BLANK

CONTENTS

EFFECTS OF ALTERNATE FUELS REPORT NO. 7: ANALYSIS OF FAIURE OF A MULLITE-BASED REFRACTORY BRICK IN AN INDUSTRIAL OIL-FIRED BURNER

J. I. Federer and V. J. Tennery

ABSTRACT

Industrial conversion from nautral gas to alternate fuels, such as residual oils and coal, often results in accelerated degradation of refractory materials due to chemical reactions with the metal impurities in the alternate fuels. Understanding how these fuel impurities affect refractory degradation reactions will improve the basis for selecting the proper refractory for industrial heating systems using alternate fuels. This report describes the cause of failure of a refractory brick used in an industrial burner firing an alternate fuel. The burner, which was used to calcine $CaSO_4$ in a lime-type kiln, was fired with No. 6 residual oil. The refractory lining in the burner was constructed of aluminosilicate brick, castable, and mortar in contact with one another. The lining deteriorated after about 1000 h, during which the maximum hot-face temperature was about 1750°C.

We subjected the degraded refractories to chemical analyses, ceramography, x-ray diffraction, scanning electron microscopy, and electron microprobe analysis. The original brick was mullite based, containing about 73% Al_2O_3 equivalent. The original castable and mortar contained only about 51 and 38% Al_2O_3, respectively. The maximum allowable service temperature of the brick was about 1790°C (about 40°C above the estimated actual service temperature). However, the maximum allowable service temperature of both the castable and mortar was only about 1550°C. Liquid phases that formed in the castable and mortar during operation of the burner at temperatures above about 1600°C reacted with the brick, resulting in decomposition of mullite. The degraded brick specimens subsequently contained about 12% CaO equivalent due to process carry-over from the kiln product and about 3% V_2O_5 equivalent and other metallic impurities from the fuel oil. Contamination of the original refractory with CaO and V_2O_5 resulted in formation of anorthite ($CaO \cdot Al_2O_3 \cdot 2SiO_2$) and aluminum vanadate ($AlVO_4$) when the contaminated refractory was cooled. Both of these compounds are less refractory than the original castable and mortar.

We conclude that failure was initiated by melting in the castable and mortar. The liquid phases attacked the adjacent brick. Contamination of the degraded brick with CaO, V_2O_5, and other impurities caused formation of compositions with much lower solidus temperatures. Consequently, large concentrations of aggressive oxide liquid were in the burner lining at the service temperature. The liquid phase eventually advanced into the refractory from the hot face to the extent that the brick grossly deteriorated. Therefore, rapid degradation of the refractory system was due to a combination of excess temperature and fluxing by process carry-over and impurities from the fuel oil.

INTRODUCTION

Natural gas shortages in U.S. industry during the winter months of 1977 emphasized the precariousness of industrial reliance on this important fuel source. In recent years a variety of industrial processes have been converted partially or completely to operate with fuels other than natural gas. These alternate fuels include distillate and residual fuel oils and coal. These fuels and the equipment required for burning them generally represent an increased cost for energy compared to that for using natural gas. The various factors involved in industrial evaluation of the conversion to alternate fuels have been discussed by Wei and Tennery.[1] Important industrial considerations are continuing availability of fuel and uninterrupted production.

Though generally less expensive than distillate oils per unit amount of energy produced, residual oils contain significantly higher concentrations of metallic impurities. These impurities, which are contained in the combustion products of oil, can degrade refractories and refractory insulations. Reports of degradation of refractories by reaction with fuel oil combustion products have become commonplace in the past 5 years. An important part of our work is analyzing industrial field samples to identify how fuel impurities affect the degradation of various refractory systems. Examination of such degraded refractories and analysis of the reaction degradation mechanisms has been the subject of six previous reports;[2–7] ours is the seventh in this series.

Of interest in our report is an aluminosilicate refractory brick used in construction of the lining of an industrial lime kiln burner fired with No. 6 residual oil. The principal crystalline phase in this refractory is mullite ($3Al_2O_3 \cdot 2SiO_2$). Mullite-based refractories have numerous applications in industrial furnace equipment, including electric arc steel furnaces, copper reverberatory furnaces, rotary cement kilns, bottom pour ladles for molten metals, and molten steel transfer cars. Our analysis strongly suggests that the refractory failure in this case was caused in part by other, less refractory materials used in construction of the burner lining, by a process contaminant, and by some of the fuel impurities.

HISTORY OF THE REFRACTORY FAILURE

The refractory failed in the combustion chamber of an oil-fired industrial burner being used to calcine $CaSO_4$ in a lime kiln. The burner, shown schematically in Fig. 1, heated the kiln for 8 h per day for about 6 months. The estimated maximum hot-face temperature of the refractories in the burner was about 1750°C. The fuel was a No. 6 residual oil, which was burned with about 15% excess air. Under these conditions the refractory lining of the combustion chamber severely degraded in about 1000 h of service.

ORNL-DWG 78-16580

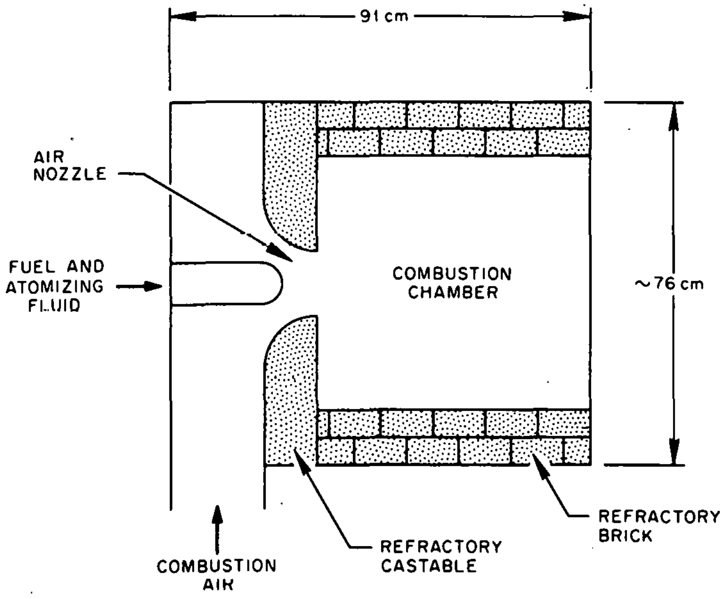

Fig. 1. Failed Oil Burner.

The burner lining, as shown in Fig. 1, consisted of three refractory materials: aluminosilicate castable located around the air nozzle, high-alumina (mullite-based) brick around the cylindrical wall, and aluminosilicate mortar for joining the bricks. The castable and some adjacent bricks deteriorated during service to the extent that detached pieces collected on the bottom of the burner. When the pieces were recovered, the original identity of the refractory from which they came could not be determined by casual inspection. However, the pieces could be separated by appearance into two groups, degraded brick and degraded castable. No effort was made by the industrial firm at the time of the failure to select or analyze identifiable samples of the refractory materials. The burner was subsequently repaired by using materials selected for greater refractoriness.

An example of the original brick is shown in Fig. 2, and pieces of the degraded brick are shown in Fig. 3. Specimens were cut or broken from pieces shown in Fig. 3 to provide samples for chemical analysis, ceramography, scanning electron microscopy, electron microprobe, and x-ray diffraction.

We investigated the degradation of the mullite-based brick, which lined the cylindrical wall of the burner chamber. Neither the castable nor the mortar were analyzed because in this case the maximum operating temperature of the burner probably far exceeded the maximum design service temperature of these materials. Therefore, their failure was probably caused by excessive service temperature (as will be discussed) rather than by reactions with oil combustion products or contamination by material fired in the kiln.

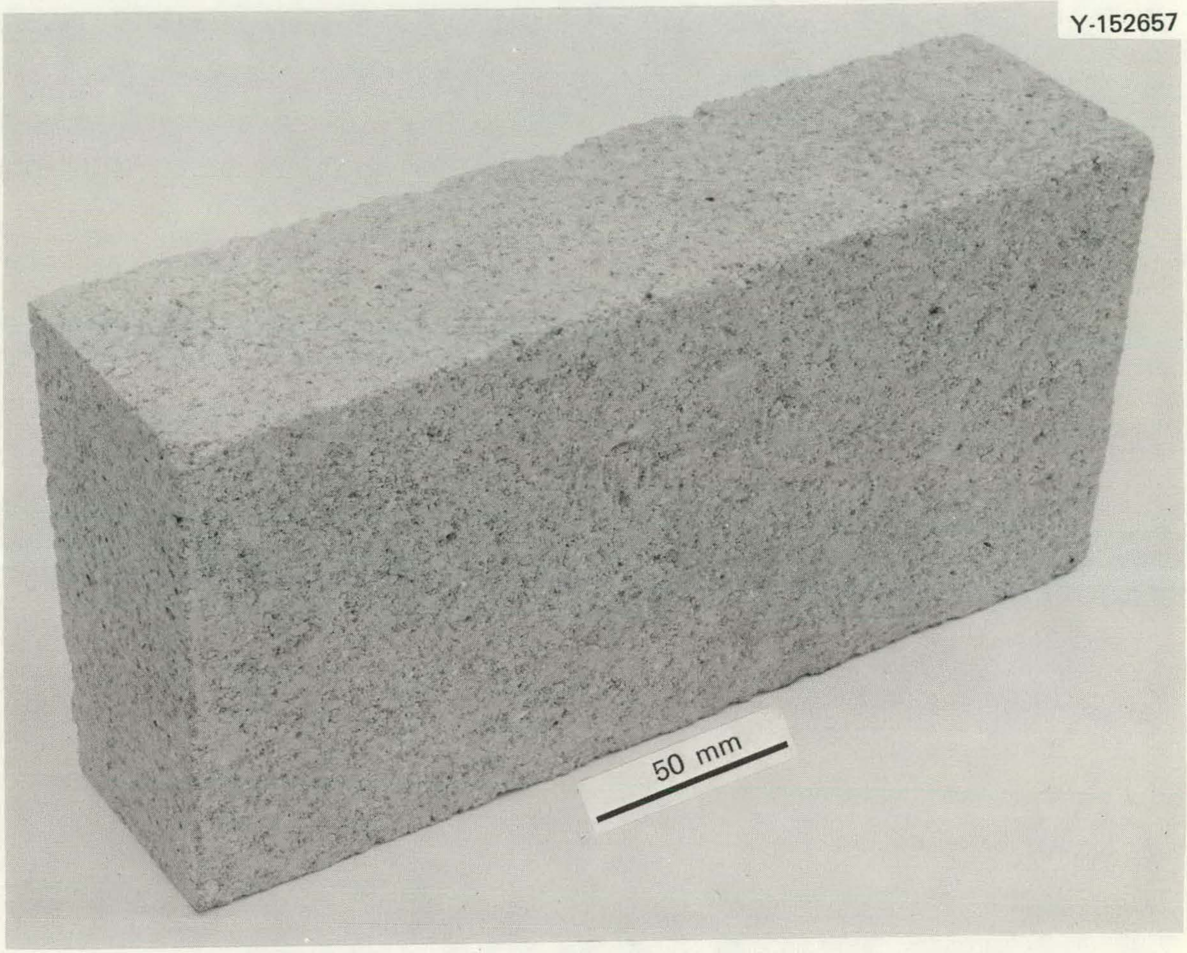

Fig. 2. Original Brick Used in Construction of the Oil Burner.

Fig. 3. Pieces of Degraded Brick.

RESULTS

Chemical Composition of the No. 6 Fuel Oil

The available chemical analysis of the No. 6 fuel oil used in the burner showed about 1.8% sulfur, 0.026% vanadium, and 0.08% ash. Since no samples of the oil were retained by the industrial user after the burner failed, a confirmation analysis of the fuel oil could not be obtained. The No. 6 oils always contain metallic impurities in amounts that depend upon the source of the crude oil and the extent of desulfurization used by the refinery. Typical metallic impurities include Ca, Fe, Na, Ni, P, Pb, Si, Zn, and V.

Analysis of the Refractory Brick

Chemical analyses of the original refractories and the degraded brick are shown in Table 1. The compositions are in oxide equivalents, which is standard practice in refractory technology. The original

Table 1. Chemical Analyses of the Original Refractories and the Degraded Brick

Element as Oxide	Concentration, wt %			
	Original Refractories			Degraded Brick
	Castable[a]	Mortar[a]	Brick	
Al_2O_3	50.85	37.50	72.64	62.58
CaO	3.14	0.14	0.13	12.04
Fe_2O_3	1.25	0.89	1.15	2.55
K_2O	0.39[b]	2.58	0.10	0.005
MgO	0.18	0.10	0.64	2.75
Na_2O			0.08	0.48
NiO				0.74
SiO_2	42.06	56.90	22.81	15.76
SrO			0.20	0.10
TiO_2	1.88	1.53	2.41	0.01
V_2O_5			0.005	2.97
LOI[c]			0.16	0.01

[a] Nominal composition supplied by manufacturer.

[b] Total alkali metal oxides.

[c] Loss-on-ignition.

castable and mortar were aluminosilicates containing about 51 and 38% Al_2O_3, respectively. The maximum allowable service temperature for these refractories is about 1550°C. The original brick was a mullite-based refractory ($3Al_2O_3 \cdot 2SiO_2$) containing about 72% Al_2O_3 and 28% SiO_2. The maximum allowable service temperature for a refractory consisting mostly of mullite is about 1790°C. The composition of the degraded brick was altered by impurities, principally calcium and vanadium and probably magnesium, sodium, and nickel also. Calcium could have been derived from the $CaSO_4$ that was being fired in the kiln, while vanadium and other impurities probably came from the fuel oil.

Crystal lattice spacings were determined by x-ray diffraction using Cu Kα radiation for the purpose of identifying phases in the original and degraded brick. The data are presented in the Appendix, and the results are summarized in Table 2. The major phases in the original brick, as determined by the diffraction line intensities, were α-alumina, mullite, sillimanite, and tridymite. The microstructure of the original brick, as shown in Fig. 4, consisted of porous grains in a glassy matrix. Figure 4(b) shows that the grains are an aggregate of randomly oriented mullite crystals, α-alumina, glass, and porosity. Table 2 shows that the degraded brick contained α-alumina, mullite, sillimanite,

Table 2. Major Crystalline Phases in the Refractory Brick

Original Brick	Degraded Brick
α-alumina, Al_2O_3	α-alumina, Al_2O_3
mullite, $3Al_2O_3 \cdot 2SiO_2$	mullite, $3\,Al_2O_3 \cdot 2SiO_2$
sillimanite, $Al_2O_3 \cdot SiO_2$	sillimanite, $Al_2O_3 \cdot SiO_2$
tridymite, SiO_2	high cristobalite, SiO_2
	anorthite, $CaO \cdot Al_2O_3 \cdot 2SiO_2$
	alumina vanadate, $AlVO_4$
	hercynite, $FeO \cdot Al_2O_3$

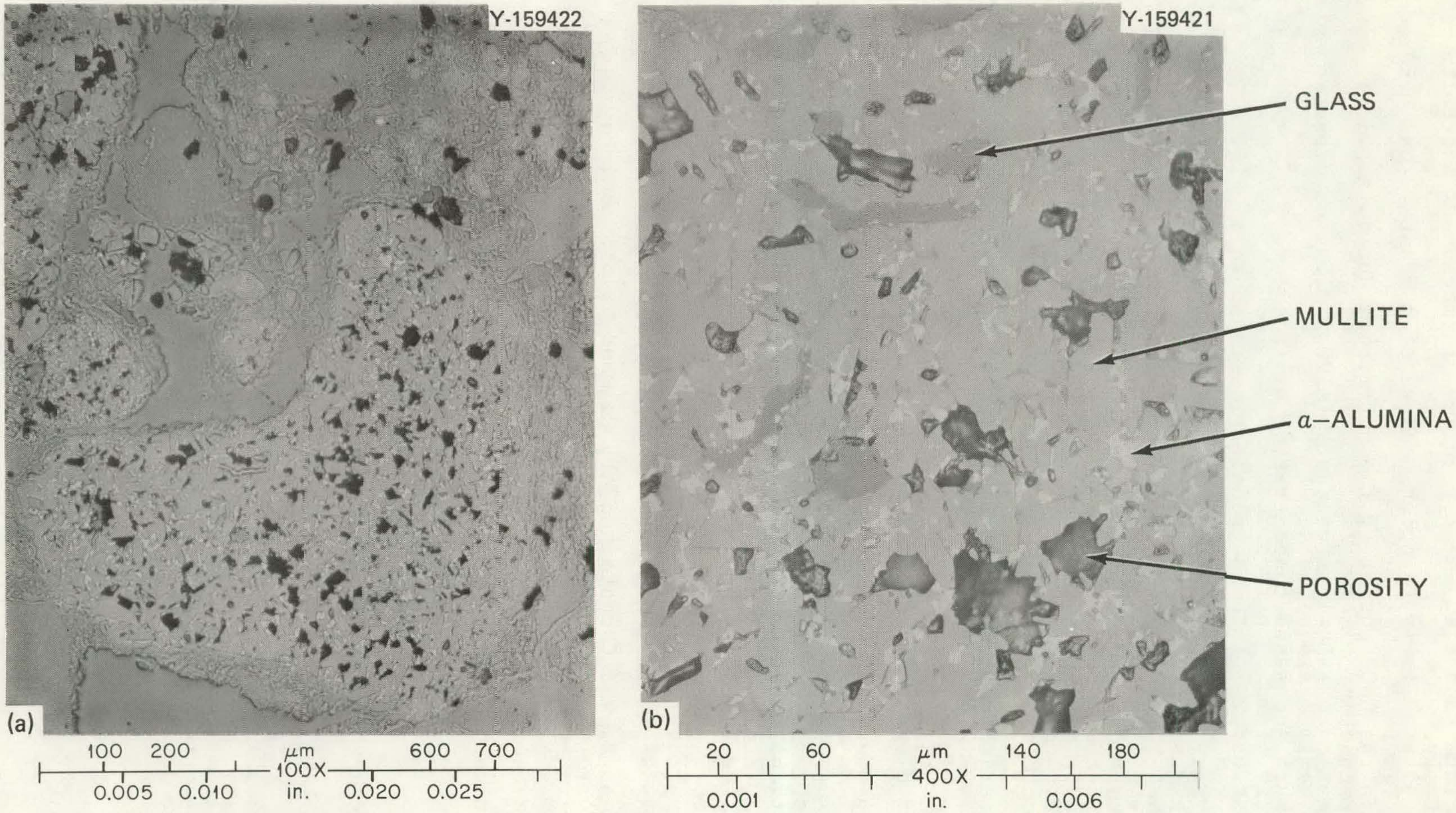

Fig. 4. Microstructure of the Original Brick. (a) Typical area showing grains in a glassy matrix. (b) Higher magnification showing that grains are an aggregate of crystals.

anorthite, aluminum vanadate, and hercynite. Formation of anorthite ($CaO \cdot Al_2O_3 \cdot 2SiO_2$) was likely to occur because of a greater than hundredfold increase in the CaO content of the refractory during service. Similarly, formation of aluminum vanadate ($AlVO_4$) might be expected as a result of the much increased concentration of vanadium.

The microstructure of the degraded brick is shown in Fig. 5. Comparison of Fig. 5 with Fig. 4 (the microstructure of the original brick) shows that the microconstituents are extensively redistributed. The microstructure of the degraded brick, shown at a higher magnification in Fig. 5(b), appears to consist of at least four phases: (1) a light-gray phase having little or no substructure; (2) another light-gray crystalline material containing porosity, possibly an aggregate of small crystals; (3) a highly reflective phase; and (4) a glassy matrix. The distribution of elements in the microstructure was determined with an electron microprobe. Characteristic x-ray energy spectra of areas A, B, and C in Fig. 5 are shown in Figs. 6, 7, and 8, respectively. The electron microprobe could not detect elements below atomic number 11; therefore, oxygen, though present in abundance, is not indicated. The information obtained with the microprobe permits determination of the location of some of the phases shown to be present by x-ray diffraction.

Each area A, B, and C contained Al, Ca, and V. Silicon, however, was found only in area C, the glassy matrix. The crystalline material in area A contained Al, Ca, and V with a small amount of Fe, making possible a mixture of α-alumina, aluminum vanadate, and possibly a calcium aluminate, although no $CaO-Al_2O_3$ phases were identified by x-ray diffraction. Area B contained Al, Ca, Fe, Mg, Ni, and V and likely consisted of a mixture of α-alumina, aluminum vanadate, hercynite, and possibly unidentified compounds containing Ca, Mg, and Ni. The glassy matrix, area C, contained Al, Ca, Si, and a small amount of V. This material probably consisted of amorphous glass, anorthite, and high cristobalite. Silicon, which was not revealed by microprobe on a polished section through the crystals, was shown by energy dispersive x-ray analysis to be present in substantial amounts on the surface of these crystals in a fracture section. We believe, therefore, that

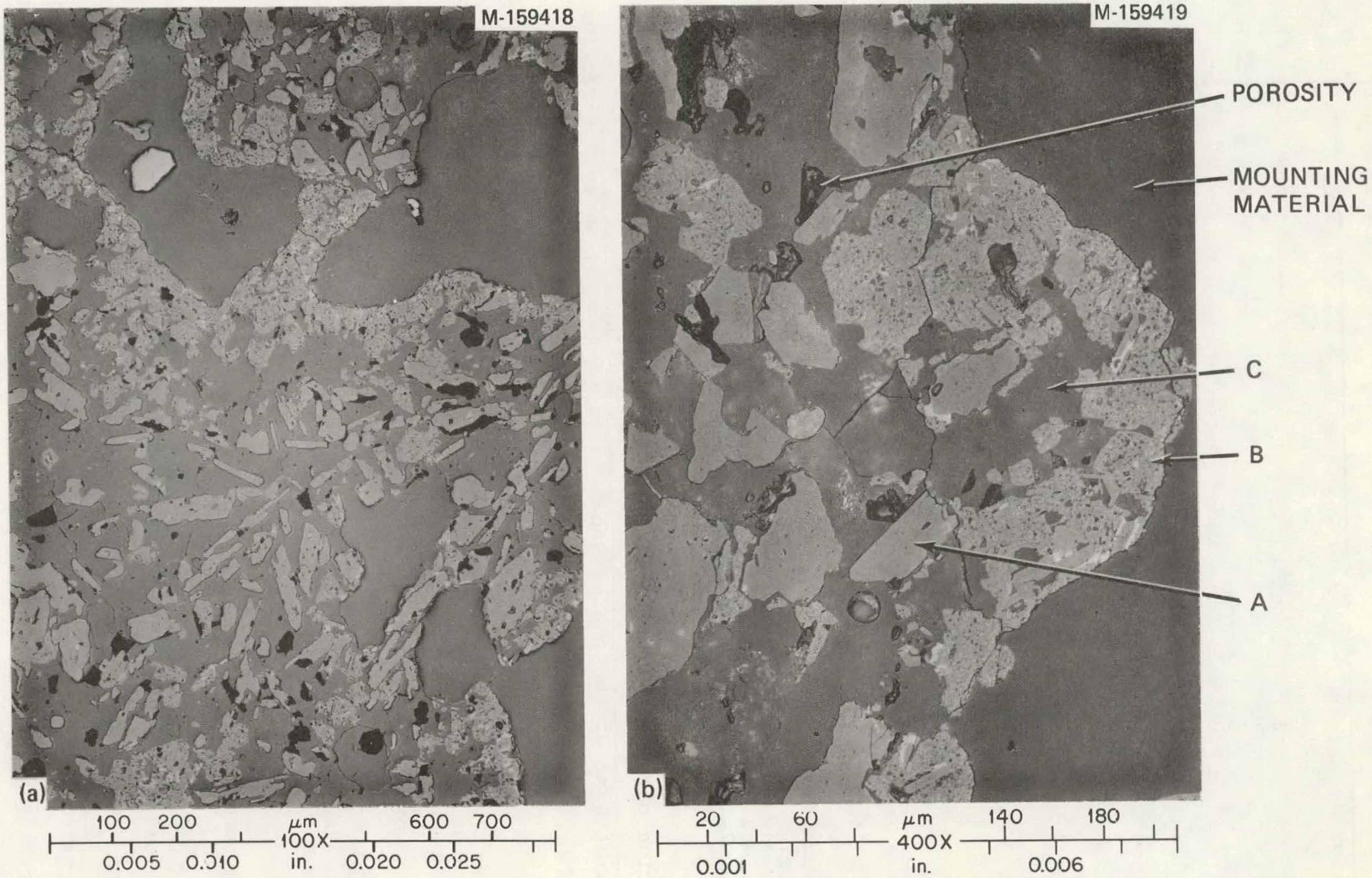

Fig. 5. Microstructure of the Degraded Brick. (a) Typical area showing crystals in a glassy matrix. (b) Higher magnification of a selected area. Phases identified: A — α-alumina and aluminum vanadate; B — α-alumina, hercynite, aluminum vanadate; C — glass containing anorthite and cristobalite.

ORNL-DWG 79-8016

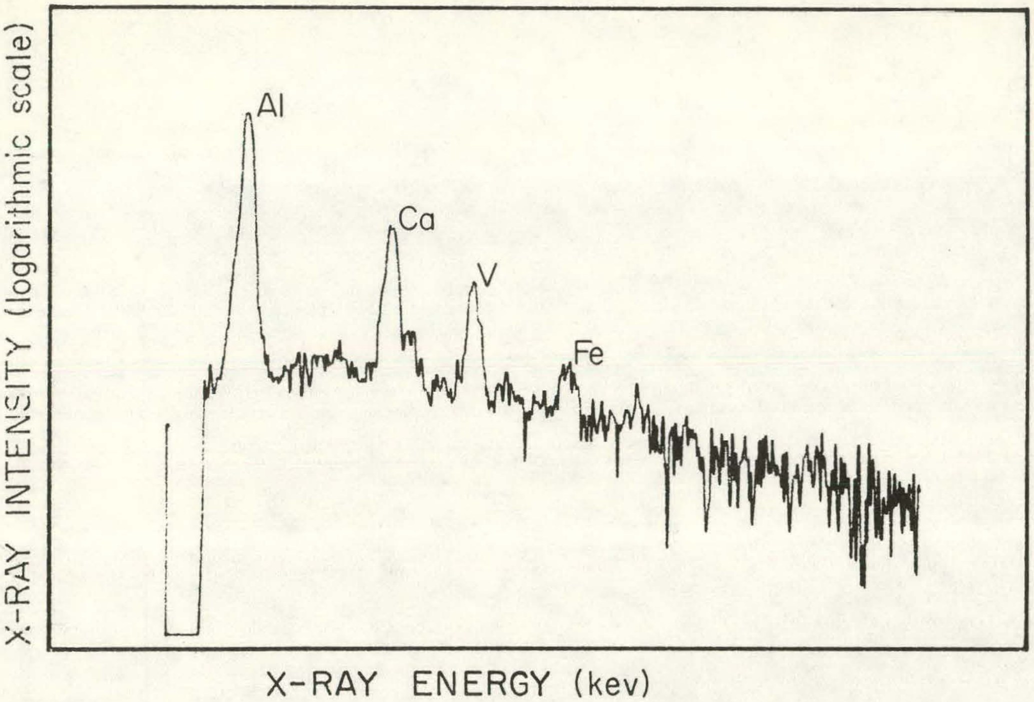

Fig. 6. Characteristic X-Ray Spectra of Area A in the Degraded Brick.

ORNL-DWG 79-8017

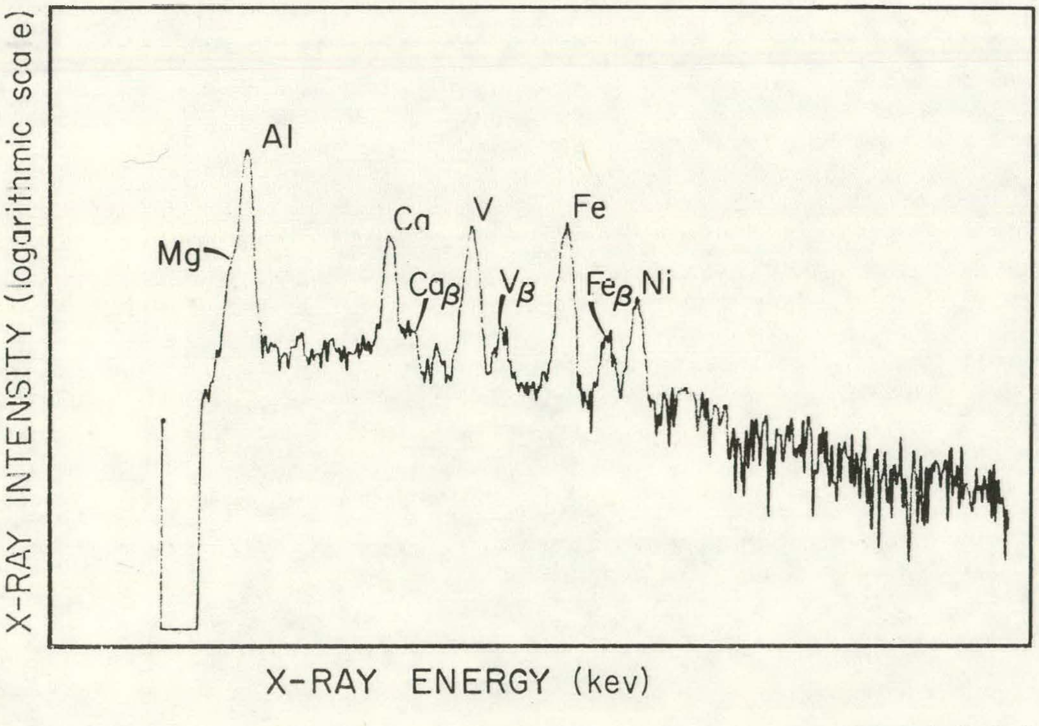

Fig. 7. Characteristic X-Ray Spectra of Area B in the Degraded Brick.

ORNL-DWG 79-8018

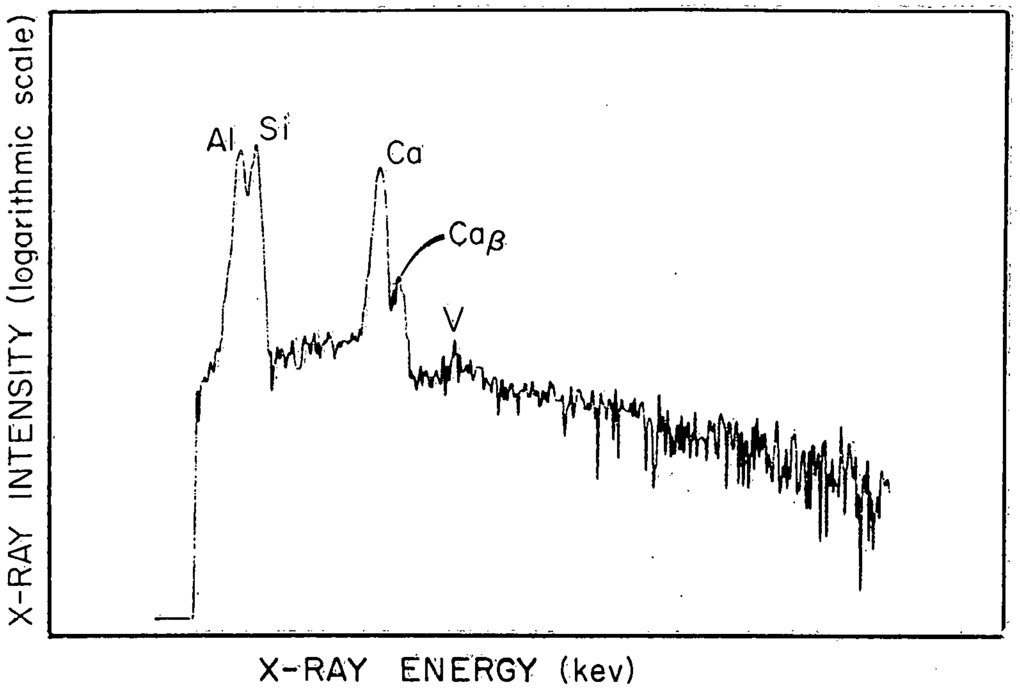

Fig. 8. Characteristic X-Ray Spectra of Area C in the Degraded Brick.

mullite occurred mainly as a relatively thin zone on the surface of α-alumina crystals. These phases could also be present as very small crystals in the silicate glass matrix.

Mullite and sillimanite were major phases in the original brick. Sillimanite, which is not stable at the high temperatures to which the refractory was exposed, would (under equilibrium conditions) decompose to mullite and cristobalite on heating.[8] The fact that mullite, in particular, was not readily identified as a discrete crystalline phase in the degraded brick suggests that this phase disassociated or dissolved in the liquid, resulting from melting of the less refractory castable and mortar. Any compositional combination of castable and/or mortar with the brick would, according to the Al_2O_3-SiO_2 phase diagram[9] shown in Fig. 9, produce a composition that would form liquid at 1590°C under equilibrium conditions. Thus, decomposition of mullite would be anticipated at the operating temperature of the burner. The new phases present after solidification of the melt would be determined by both the composition of the melt and the approach to equilibrium during cooling.

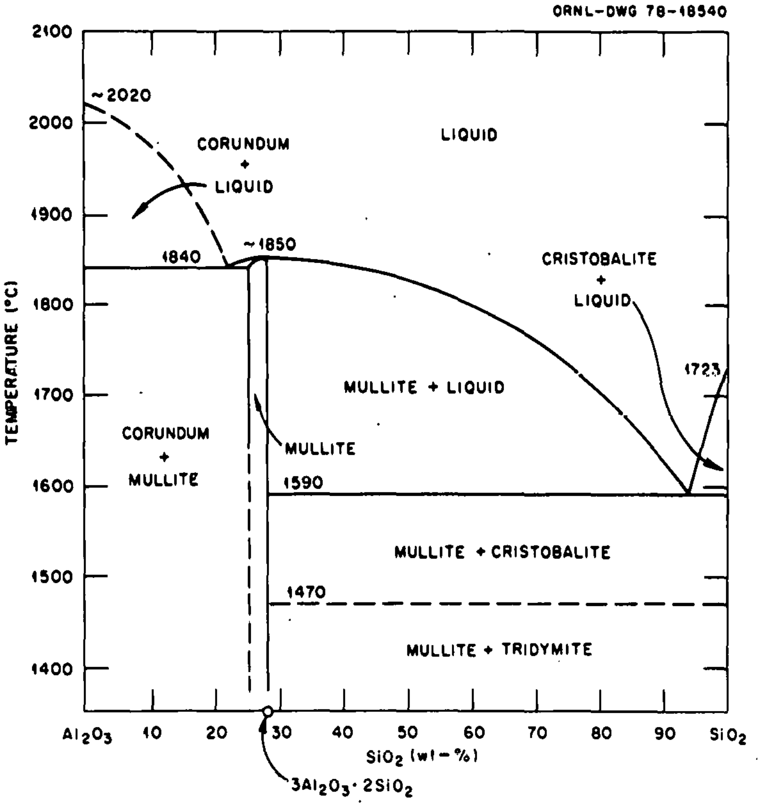

Fig. 9. The Al_2O_3-SiO_2 Phase Diagram.

DISCUSSION

The original castable refractory and mortar, while not subjects of this report, may have been largely responsible for failure of the refractory brick in the burner lining. The original castable was an aluminosilicate containing about 50% Al_2O_3 (oxide equivalent). The original mortar, also an aluminosilicate, contained about 38% Al_2O_3. According to the Al_2O_3-SiO_2 phase diagram[9] shown in Fig. 9, compositions containing less than about 72% Al_2O_3 form a liquid phase when heated above 1590°C. The industrial user of the failed oil burner estimated that a maximum temperature of 1750°C was attained at the hot face during service. At this temperature the castable and mortar would consist of at least 50% liquid, which would be structurally unstable. The actual amount of liquid generated would be determined by the amount of impurity oxides present and the extent to which equilibrium was approached. On the other hand, the original brick, which contained about 73% Al_2O_3, would have contained no liquid phase below about 1840°C. We believe, therefore, that the refractory system failure was initiated by melting of the castable and mortar components of the structure. This liquid phase resulted in dissolution of the brick. At the same time the mullite-based refractory was contaminated by calcium from the calcining process and by impurities in the fuel oil used to fire the kiln. Contamination with calcium and vanadium was particularly detrimental as these impurities resulted in formation of compounds and melts even less refractory than the original castable and mortar compositions. Anorthite ($CaO \cdot Al_2O_3 \cdot 2SiO_2$) melts at about 1550°C, and aluminum vandate ($AlVO_4$) melts at about 640°C.

The principal oxide equivalent components of the degraded brick were Al_2O_3, SiO_2, and CaO. The normalized concentrations of these oxides (neglecting other oxides) are 69% Al_2O_3, 18% SiO_2, and 13% CaO. An examination of the Al_2O_3-SiO_2-CaO phase diagram[10] in Fig. 10 reveals that this composition lies within a field consisting of alumina, anorthite, and hibonite ($CaO \cdot 6Al_2O_3$) at the temperatures of interest. We cannot explain why hibonite was not found by x-ray diffraction despite the fact that calcium was found in each of the three microstructural areas analyzed with the electron microprobe. This may be due to lack of attainment of phase equilibrium, or possibly the presence of vanadium in relatively small amounts prevents the appearance of hibonite.

A possible scenario is one in which the oil-fired burner was heated daily to a temperature that was marginally safe for the castable and mortar or perhaps exceeded their maximum service temperatures. Liquid phases, once formed, were contaminated with impurities from the kiln contents and from fuel oil impurities. This contamination resulted in a lowering of the temperature at which significant amounts of liquid phase were generated. During subsequent heating the liquid continued to react with the more refractory mullite phase. The reaction zone progressed further into the bulk refractory until the brickwork structure physically collapsed.

ORNL-DWG 79-10297

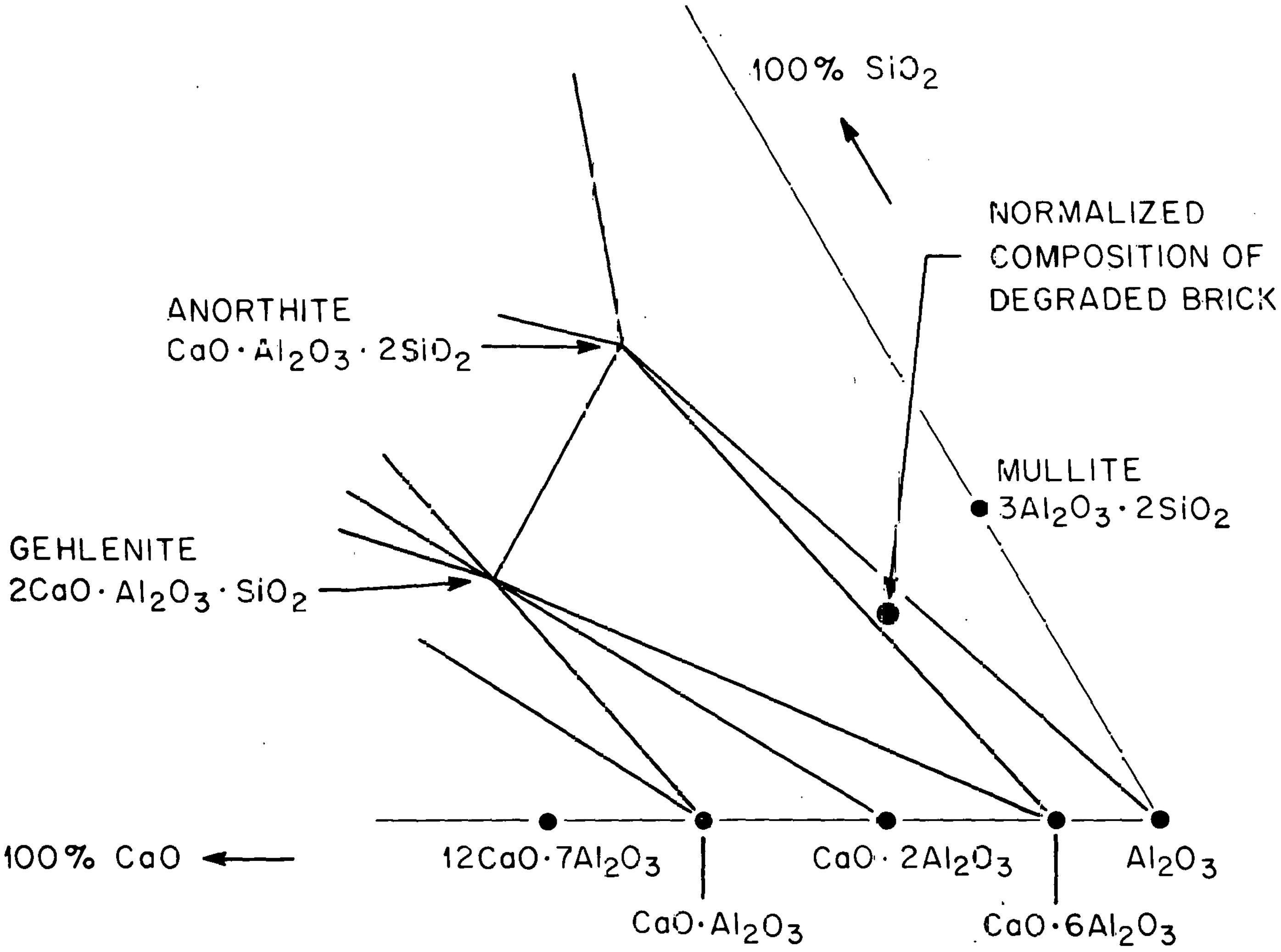

Fig. 10. A Portion of the Al_2O_3-SiO_2-CaO Phase Diagram.

CONCLUSIONS

Results of our analyses permit the following conclusions regarding failure of the refractory bricks from the lime kiln industrial burner fired with No. 6 fuel oil.

1. The brick used in construction of the burner lining was a mullite-based composition with a maximum allowable service temperature of about 1790°C.
2. The castable refractory and refractory mortar also used in construction of the burner lining were aluminosilicates with considerably lower allowable service temperatures than the brick.
3. Significant portions of the castable and mortar melted when the burner was operated at a maximum temperature of about 1750°C.
4. Formation of liquid phases in the castable and mortar, all of which were in contact with the brick, contributed to dissolution of the brick.
5. The refractories were heavily contaminated by CaO from the kiln product and by V_2O_5 and other impurities from the fuel oil.
6. Contamination of the refractory system with calcium and vanadium resulted in formation of calcium and vanadium compounds with even lower solidus temperatures than the original refractories. This caused significant quantities of liquid phase to be produced at relatively low temperatures.
7. Reaction and dissolution of the mullite-based brick by these liquids caused extensive degradation of the brick, finally resulting in complete loss of its physical integrity.

ACKNOWLEDGMENTS

The authors wish to acknowledge the contributions of others to the completion of this work: J. W. Greer, sample preparation; W. H. Warwick, ceramography; T. J. Henson and R. S. Crouse, electron microprobe; and O. B. Cavin, x-ray diffraction. We thank T. N. Tiegs and T. G. Godfrey for their critical review and comments, B. G. Ashdown for editorial assistance, and K. A. Witherspoon for preparing the report for publication.

REFERENCES

1. G. C. Wei and V. J. Tennery, *Impact of Alternate Fuels on Industrial Refractories and Refractory Insulation Applications*, ORNL/TM-5592 (September 1976).
2. G. C. Wei, L. A. Harris, and V. J. Tennery, *Effects Of Alternate Fuels, Report No. 1, Analysis of High-Duty Fireclay Refractories Exposed to Coal Combustion*, ORNL/TM-5909 (December 1977).
3. G. C. Wei and V. J. Tennery, *Effects of Alternate Fuels, Report No. 2, Analysis of Basic Refractories Degraded by Residual Oil Combustion Products*, ORNL/TM-6088 (February 1978).
4. G. C. Wei and V. J. Tennery, *Effects of Alternate Fuels, Report No. 3, Analysis of High-Duty Fireclay Refractories Degraded by Residual Oil Combustion Products*, ORNL/TM-6184 (April 1978).
5. G. C. Wei and V. J. Tennery, *Effects of Alternate Fuels, Report No. 4, Analysis of Soaking Pit Cover Refractories Degraded by Residual Oil Combustion Products*, ORNL/TM-6204 (April 1978).
6. G. C. Wei and V. J. Tennery, *Effects of Alternate Fuels, Report No. 5, Analysis of Fused Cast AZS Refractory, Silica Refractory, and High-MgO Refractory Degraded by Residual Oil Combustion Products*, ORNL/TM-6278 (April 1978).
7. G. C. Wei and V. J. Tennery, *Effects of Alternate Fuels, Report No. 6, Analysis of Low-Alumina Castable Refractory Degraded by Residual Oil Combustion Products*, ORNL/TM-6334 (July 1978).
8. E. Ryshkewitch, *Oxide Ceramics*, Academic Press, New York, 1960.
9. E. M. Levin, C. R. Robbins, and H. F. McMurdie, *Phase Diagrams for Ceramists*, The American Ceramic Society, Columbus, Ohio, 1964, p. 123.
10. E. M. Levin, C. R. Robbins, and H. F. McMurdie, *Phase Diagrams for Ceramists*, The American Ceramic Society, Columbus, Ohio, 1964, p. 219.

APPENDIX

Lattice Spacings of Phases in Both the Original and Degraded Brick Determined by X-Ray Diffraction

THIS PAGE

WAS INTENTIONALLY

LEFT BLANK

Table A-1. Phases in the Original Brick Determined by X-Ray Diffraction

Lattice Spacing, nm				
Original Brick	Mullite $3Al_2O_3 \cdot 2SiO_2$	α-Alumina Al_2O_3	Sillimanite $Al_2O_3 \cdot SiO_2$	Tridymite SiO_2
0.53466	0.539		0.535	
0.47125				
0.45291			0.456	
0.42442				0.4236
0.40804				0.4107
0.37540	0.3774		0.373	0.3818
0.34623		0.3479		0.3461
0.34140	0.3428		0.341	0.3396
0.33759	0.3390		0.336	
0.31512			0.319	0.3171
0.28792	0.2886		0.288	
0.26873	0.2694		0.267	
0.25446	0.2542	0.2552	0.253	0.2540
0.25081				0.2500
0.24232	0.2428		0.242	0.2385
0.23751	0.2393	0.2379	0.237	0.2342
0.22897	0.2292		0.228	0.2294
0.22048	0.2206		0.220	0.2205
0.21600		0.2165		0.2137
0.21179	0.2121			0.2117
0.21024	0.2106		0.210	
0.20817		0.2085	0.209	0.2086
0.19609	0.1969	0.1964	0.1959	
0.19225	0.1923			0.1943
0.19058				0.1905
0.18846	0.1887		0.1868	0.1874
0.18399	0.1841		0.1829	0.1829
0.17949	0.17954		0.1783	0.1783
0.17365		0.1740		
0.17127	0.17125			0.1715
0.16998	0.17001		0.1705	
0.16937	0.16940		0.1690	0.1695
0.16007	0.15999	0.1601	0.1595	0.1600
0.15784	0.15786			
0.15655	0.15644		0.1567	
0.15465	0.15461	0.1546	0.1559	0.1546
0.15248	0.15242		0.1535	0.1530
0.15148		0.1514	0.1516	0.1517
0.15093	0.15067	0.1510		0.1510
0.14894				0.1488
0.14860	0.14811			
0.14598	0.14605		0.1467	0.1467
0.14503			0.1450	
0.14441	0.14421		0.1440	0.1443
0.14347				0.1434
0.14250	0.14240		0.1418	0.1413
0.14035	0.14046	0.1404	0.1392	0.1402
0.13725		0.1374		
0.13472			0.1343	
0.13355		0.1337	0.1337	

Table A-2. Phases in the Degraded Brick Determined by X-Ray Diffraction

Lattice Spacing, nm							
Degraded Brick	α-Alumina Al_2O_3	Mullite $3Al_2O_3 \cdot 2SiO_2$	Sillimanite $Al_2O_3 \cdot SiO_2$	High Cristobalite SiO_2	Anorthite $CaO \cdot Al_2O_3 \cdot 2SiO_2$	Aluminum Vandate $AlVO_4$	Hercynite $FeO \cdot Al_2O_3$
0.64917					0.652		
0.48113						0.494	
0.46952					0.469		0.469
0.46586							
0.44950						0.433	
0.41520				0.415		0.429	
0.40311					0.404		
0.39273					0.392		
0.37792		0.3774			0.378	0.373	
0.36158					0.362	0.359	
0.34742	0.3479				0.348	0.346	
0.34282		0.3428			0.346		
0.34012		0.3390	0.341		0.340	0.340	
0.33597			0.336		0.336	0.338	
0.32831					0.326		
0.32619							
0.32090					0.321	0.320	
0.32022					0.319		
0.31865			0.319		0.318	0.317	
0.31178					0.312	0.310	
0.30789						0.307	
0.30379					0.304	0.303	
0.29308			0.293	0.292	0.2934	0.297	
0.28847		0.2886	0.288		0.2893	0.2873	0.287
0.26595		0.2694	0.267		0.2655	0.2682	
0.25470	0.2552	0.2542	0.253	0.253	0.2559	0.2527	
0.24346		0.2428	0.242		0.2437	0.2460	0.245
0.23860	0.2379	0.2393	0.237		0.2384	0.2361	
0.22378		0.2292	0.228		0.2239		
0.22023		0.2206	0.220	0.217			
0.21438	0.2165	0.2121			0.2143	0.2161	
0.21146		0.2106	0.210		0.2118		
0.20904	0.2085		0.209	0.207	0.2095	0.2076	
0.20170			0.1980	0.199	0.2016	0.2017	0.202
0.19649	0.1964	0.1969	0.1959			0.1946	
0.19263		0.1923				0.1897	
0.18813		0.1887					
0.18682		0.1863	0.1868				
0.18372		0.1841	0.1829			0.1835	
0.17972		0.17954	0.1807	0.1795		0.1806	
0.17649			0.1783				
0.17414	0.1740						
0.17181		0.17125	0.1705			0.1727	
0.16819		0.16940	0.1679	0.169			
0.16474				0.1641		0.1626	0.164
0.16035	0.1601	0.15999	0.1595			0.1598	
0.15550		0.15644	0.1559				0.156
0.15472	0.1546	0.15461					
0.15371			0.1535				
0.15126	0.1514	0.15242	0.1516			0.1510	
0.15003		0.15067					
0.14758		0.14811	0.1467				
0.14560		0.14605		0.1460			
0.14463		0.14421	0.1450				
0.14269		0.14240	0.1440				0.143
0.14067	0.1404	0.14046	0.1418				
0.13760	0.1374		0.1392	0.1380			
0.13207			0.1337				
0.12991							
0.12777	0.1276			0.1266			
0.12406	0.1239						0.123
0.12113				0.1210			
0.11907	0.11898						
0.11662	0.11600						0.117
0.11503							
0.11476	0.11470						
0.11450	0.11382						
0.11263	0.11255			0.1131			
0.11002	0.10988						
0.10855	0.10831			0.1090			
0.10800	0.10781						0.108
0.10505							0.105
0.10451	0.10426						

ORNL/TM-6878

INTERNAL DISTRIBUTION

1–2. Central Research Library
3. Document Reference Section
4–5. Laboratory Records Department
6. Laboratory Records, ORNL R.C.
7. ORNL Patent Section
8. R. A. Bradley
9. J. V. Cathcart
10. R. G. Donnelly
11–20. J. I. Federer
21. T. G. Godfrey
22–24. M. R. Hill
25. W. J. Lackey
26. A. E. Pasto
27. A. C. Schaffhauser
28. J. E. Selle
29–43. V. J. Tennery
44. G. C. Wei
45. R. W. Balluffi (Consultant)
46. A. L. Bement, Jr. (Consultant)
47. W. R. Hibbard, Jr. (Consultant)
48. E. H. Kottcamp, Jr. (Consultant)
49. M. J. Mayfield (Consultant)
50. J. T. Stinger (Consultant)

EXTERNAL DISTRIBUTION

51. D. Allen
Southwestern Portland Cement Co.
P.O. Box 937
Victorville, CA 92305

52. R. W. Anderson
Diversified Insulation, Inc.
P.O. Box 188
Hamel, MI 55340

53. N. Ault
Norton Company
One New Bond Street
Worcester, MA 01606

54. J. E. Bailey
Raw Materials Specialist
Ford Motor Company
Glass Technical Center
25500 West Outer Drive
Lincoln Park, MI 48146

55. B. H. Baker
Armco Steel Corp.
Res. Center South
Middletown, OH 45043

56. W. T. Bakker
Div. of Systems Engineering/
Energy Technology
Department of Energy
Rm. C-157
Germantown, MD 20767

57. L. Baumer
Ownes-Illinois, Inc.
P.O. Box 1035
Toledo, OH 43666

58. I. W. Bjerklie
Hague International
3 Adams Street
South Portland, MA 04106

59. J. M. Bevilacqua
The Carborundum Co.
P.O. Box 808
Niargara Falls, NY 14302

60. D. R. Bissel
Drexel Refractories Co.
Box 50
Kittaning, PA 16201

61. D. S. Blum
Quality Control Manager
Plibrico Company
1800 N. Kingsbury Street
Chicago, IL 60614

62. G. E. Brinkerhoff
Manager, Technical Services
A. P. Green Refractories
Company
Mexico, MO 65265

63. J. J. Brown
Dept. of Materials
Engineering
Virginia Polytechnic
Institute and State
University
Blacksburg, VA 24061

64. B. R. Brown
E. I. DuPont de Nemours
& Co., Inc.
1007 Market St.
Wilmington, DE 19898

65. F. Campbell
Babcock and Wilcox Co.
Box 923
Old Savanna Rd.
Augusta, GA 30903

66. J. A. Crookston
A. P. Green Refractories Co.
Green Blvd.
Mexico, MO 65265

67. J. Eustis
Division of Industrial
Energy Conservation
Department of Energy
20 Massachussetts Ave., NW
Washington, DC 20545

68. W. X. Fay
General Refractories Co.
50 Monument Rd.
Bala-Cynwyd, PA 19004

69. M. P. Fedock
Assistant Division Head
Iron and Steelmaking Division
Republic Steel Corporation
Research Center
6801 Brecksville Road
Cleveland, OH 44131

70. Robert A. Fenimore
ICI Americas, Inc.
Specialty Chemicals Division
Wilmington, DE 19849

71. L. E. Ferreira
Interpace Corporation
Corporate Headquarters
Box 1111
Parsippany, NJ 07054

72. R. E. Ferris
Kaiser Research Center
Box 870
Pleasanton, CA 94566

73. R. Grekrila
Research Center
Westinghouse Electric Corp.
Beulah Road
Pittsburgh, PA 15235

74. R. S. Harris
Anchor Hocking Company
Lancaster, OH 43135

75. D. Harvey
Department of Energy
20 Massachusetts Ave., NW
Washington, DC 20545

76. R. H. Herron
Homer Research Laboratory
Bethlehem Steel Corporation
Bethlehem, PA 18017

77. A. V. Illyn
Babcock & Wilcox
P.O. Box 923
Augusta, GA 30903

78. H. L. Johns
Zircoa Products
31501 Solon Road
Solon, OH 44139

79. K. K. Kappmeyer
Applied Research Laboratory
United States Steel Corp.
Monroeville, PA 15146

80. W. D. Kingery
Department of Materials
Science and Engineering
Massachusetts Institute of
Technology
Cambridge, MA 02139

81. L, Krietz
Plibrico Company
1800 N. Kingsbury Street
Chicago, IL 60614

82. L. J. Kuhlman
Monsanto Company
800 N. Lindberg Blvd.
St. Louis, MO 63166

83. R. G. LaBar
Alcoa Research Laboratories
Aluminum Company of America
Alcoa Center, PA 15069

84. R. A. Landy
Director of Research
North American Refractories
Company Research Center
Curwensville, PA 16833

85. J. Langensiepen
Brockway Glass Company
Central Laboratory
Brockway, PA 15824

86. R. Limes
Republic Steel Corporation
1441-T Republic Bldg.
P.O. Box 6778
Cleveland, OH 44101

87. C. Lindsay
Tennessee Valley Authority
303 Union Bldg.
Knoxville, TN 37902

88. D. E. McBride
Zircoa
31501 Solon Rd.
Box 39217
Solon, OH 44139

89. J. R. McGaughey
Bickley Furnaces, Inc.
550 State Road
Philadelphia, PA 19114

90. T. D. McGee
Iowa State University
Materials Science and
Engineering Department
Ames, IA 50010

91. R. W. Marshell
North American Manufacturing
Company
4455 E. 71st Street
Cleveland, OH 44105

92. F. M. Maupin
A. P. Green Refractories
Company
Green Blvd.
Mexico, MO 65265

93. W. Mead
Temtek-Allied Division
Ferro Corp.
One Erieview Place
Cleveland, OH 44114

94. R. J. Moffat
Pullman-Swindell
441 Smithfield Street
Pittsburgh, PA 15222

95. R. Neeley
Chattanooga Glass Company
400 W. 45th Street
Chattanooga, TN 37410

96. J. A. Nelson
University of Illinois
Urbana, IL 61801

97. R. E. Nelson
C-E Minerals Company
901 E. 8th Avenue
King of Prussia, PA 19406

98. T. H. Nielsen
Coors Porcelain Company
600 9th Street
Golden, CO 80401

99. D. Olenchut
Jones and Laughlin Steel Corp.
3A, Gateway Center
Pittsburgh, PA 15230

100. H. Orr
Trane Thermal Company
Brook Road
Conshohocken, PA 19428

101. J. Osborne
Division of Industrial
Energy Conservation
Department of Energy
20 Massachusetts, Ave., NW
Washington, DC 20545

102. R. C. Oxford
Development Laboratory
Refractories Division
Babcock & Wilcox Company
P.O. Box 923
Augusta, GA 30903

103. P. Papa
Cornhart Refractories Co.
1600 W. Lee Street
Louisville, KY 40210

104. J. D. Parsons
Chicago-Wellsville Fire
Brick Company
1467 Elston Ave.
Chicago, IL 60622

105. C. M. Pelanne
Johns-Manville Corp.
Box 5108
Denver, CO 80217

106. M. Perlsweig
Fuel Utilization Division
Fossil Energy
E 178
Department of Energy
Washington, DC 20543

107. G. V. Prible
C-E Refractories Co.
(Div. of Combustion
Engineering, Inc.)
Box 828
Valley Forge, PA 19482

108. R. Ramey
Inland Steel Research
3001 East Columbus Drive
East Chicago, IN 46312

109. R. Rose
H. K. Porter Co.
Porter Bldg.
601 Grant St.
Pittsburgh, PA 15219

110. R. P. Ross
Glasrock Products, Inc.
2210 Marietta Blvd., NW
Atlanta, GA 30318

111. G. R. Rowland
Hartford Refractories,
Emhart Corp.
P.O. Box 2809
Hartford, CT 06101

112. C. K. Russell
Res. Center
United States Steel Corp.
125 Jamison Lane
Mail Stop 43
Monroeville, PA 15146

113. B. L. Schmidt
Anchor Hocking Co.
Lancester, OH 43130

114. F. E. Schmidt
E. I. DuPont de Nemours & Co., Inc.
Experimental Stations
Bldg. 304
Wilmington, DE 14898

115–119. R. Sheneman
High Temperature Processes Branch
Department of Energy
20 Massachusetts Ave.
Washington, DC 20585

120. R. L. Shultz
Armco Steel Corp.
Research Center South
Middletown, OH 45043

121. W. J. Smothers
Homer Res. Labs.
Bethlehem Steel Corp.
Bethlehem, PA 18016

122. R. R. Smyth
FluiDyne Engineering Co.
5900 Olson Memorial Highway
Minneapolis, MN 55422

123. L. H. Sweet
Manager Technical Development
Carborundum Co.
P.O. Box 808
Niagara Falls, NY 14302

124. C. A. Taylor
Shell Oil Co.
1 Shell Plaza, Box 2463
Houston, TX 77001

125. W. H. Thielbahr
Idaho Operations Office
Department of Energy
Idaho Falls, Idaho 83401

126. E. A. Thomas
Charles Taylor Div.
NL Industries, Inc.
8361 Broadwell Road
P.O. Box 44040
Cincinnati, OH 45244

127. L. J. Trostel, Jr.
Norton Co.
One New Bond St.
Worcester, MA 01606

128. B. S. Tucker
The Refractories Inst.
1102 One Oliver Plaza
Pittsburgh, PA 15222

129. M. L. Van Dreser
Center for Technology
Kaiser Aluminum and Chemical Corp.
Box 870
Pleasanton, CA 94566

130. R. F. Whitford
North American Refractories Co.
1012 National City E 6th Bldg.
Cleveland, OH 44114

131. J. R. Wilson
Shell Development Co.
Box 1380
Houston, TX 77001

132. J. Wosinsky
Corning Glass Works
Box 432
Corning, NY 14830

133. R. L. Yeckley
Industrial Market
Harbison-Walker Refractories
Division of Dresser Industries, Inc.
2 Gateway Center
Pittsburgh, PA 15222

134. S. Young
Babcock and Wilcox Refractories Co.
Old Savanna Rd
Box 923
Augusta, GA 30903

135. C. E. Zimmer
Babcock and Wilcox Co.
Lynchburg, VA 24505

136. Assistant Manager
Energy Research and Development
Department of Energy
Oak Ridge Operations Office
P.O. Box E
Oak Ridge, TN 37830

137–163. Department of Energy
Technical Information Center
Office of Information Services
P.O. Box 62
Oak Ridge, TN 37830